2017 IEEE International Conference on Robotics and Automation (ICRA)
Singapore, May 29 - June 3, 2017

Between-Leg Coupling Schemes for Passively-Adaptive Non-Redundant Legged Robots

Oren Y. Kanner, *Student Member, IEEE*, Nicolas Rojas, *Member, IEEE*, and Aaron M. Dollar, *Senior Member, IEEE*

***Abstract*— This paper studies the synthesis of between-leg coupling schemes for passively-adaptive non-redundant legged robots. Highly actuated legged robots can arbitrarily locate their feet relative to their bodies through active control, but often wind up kinematically over-constrained following ground contact, requiring complex redundant control for stable locomotion. The use of passive sprung joints can provide some minimal passive adaptability to terrain, but it is limited to relatively low terrain variability due to practical travel limits. In this paper, using a 4-RR platform as case study, we show that implementing parallel adaptive couplings between legs of a stance platform can yield substantial passive adaptability to rough terrain while still ensuring that the body is fully constrained in stance. This study uses screw theory-based mobility analysis methods to determine the number of constraints required to control the stance platform. Several coupling schemes are then considered and evaluated through a simulation of their stance capabilities over arbitrary terrain. An experimental validation of these simulation results is presented; it demonstrates the viability of the proposed scheme for passive adaptability.**

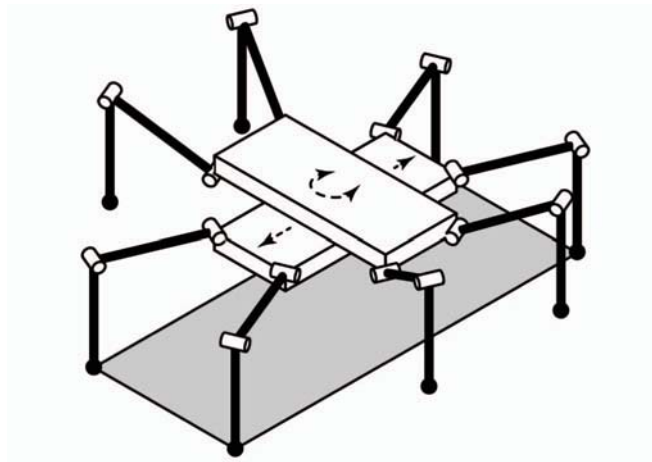

Figure 1. Illustration of 3-DOF walking robot, consisting of two identical 1-DOF stance platforms connected by a 2-DOF mechanism permitting the motions indicated by the arrows. The static support polygon is indicated in gray.

I. INTRODUCTION

Designing robotic systems to interact with unstructured environments is a difficult challenge, all the more so when that environment is entirely unknown. Legged robots do offer the potential for successful locomotion over uneven terrain due to their use of sets of discrete contact points to support themselves and the ability to lift their legs over obstacles and other terrain discontinuities. Multi-legged walking robots, i.e. those that ensure static stability at all times, can additionally offer control over the position and posture of the body to some extent. These robots often utilize complex multi-degree-of-freedom (DOF) legs with multiple actuators to precisely control the position of the feet relative to the body [1]. However, such robots can end up over-constrained once the feet are in contact with the ground, potentially leading to destabilizing reaction forces or a loss of contact, which can further lead to a loss of static stability. As a consequence, they require complex active control to ensure that all feet are in contact with the ground in stance [2], [3].

Passive adaptability allows robots to interact with their environments in an open-loop manner. Some robots use passive compliant suspensions to allow for terrain variability and reduce over-constraint [4]–[6], but this only provides limited adaptability to arbitrarily terrain due to practical travel limits. In manipulation, passive adaptability has been achieved through the use of underactuatated differential mechanisms [7], leading to robust open-loop grasping of arbitrarily shaped objects. We aim to apply the same principles to legged locomotion. Moreover, by avoiding actuator redundancy and minimizing the number of actuators in the robot, we design systems that are cheaper, lighter, and simpler to control [8]. This approach would be particularly suited to power-constrained environments with high terrain variability, such as extraterrestrial exploration or disaster recovery. This paper studies the synthesis of different actuation schemes for adaptive legged robots and their effect on stance performance, using a 4-RR platform as case study (Fig. 1).

There are numerous ways to distribute actuator effort between multiple joints / legs. Direct couplings such as gear trains or linkages define fixed relationships between the actuator position and some set of joints in the system. This can be used to mechanically specify that a set of legs should move together, e.g. for an alternating tripod gait [9]. Some researchers have used hydraulics / pneumatics or equivalent systems to distribute a force input across multiple joints [10]. We elected to implement a differential position control through tendon couplings, similar to the design of the SDM hand and previously discussed in [11]. Moreover, by

Research sponsored in part by the National Science Foundation grant IIS-1637647.

O. Y. Kanner and A. M. Dollar are with the Department of Mechanical Engineering and Materials Science, Yale University, New Haven, CT 06520 USA (e-mails: oren.kanner@yale.edu, aaron.dollar@yale.edu).

N. Rojas is with the Dyson School of Design Engineering, Imperial College London, London, UK (e-mail: n.rojas@imperial.ac.uk).

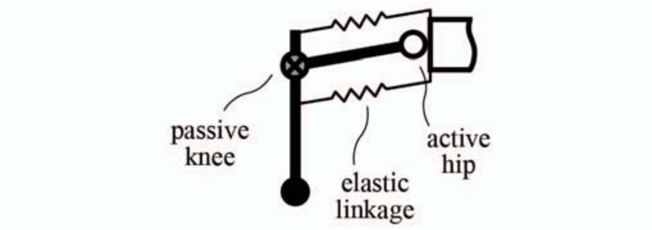

Figure 2. Illustration of the 2-RR leg used in this design, entirely controlled through the hip angle with the knee passive.

combining independent couplings in parallel we can exert multiple constraints with a single actuator and maintain control simplicity.

The rest of the paper is organized as follows. Section II describes the adaptive legged robot design that serves as case study. Section III presents a screw theory-based analysis of the mobility of the adaptive stance platform and several actuation schemes that could be used to control it. A numerical simulation used to evaluate the stance performance of the different actuation schemes is described in Section IV. Section V shows an experimental validation of the simulation, and we conclude in Section VI.

II. 4-RR Stance Platform Design

Fig. 1 shows a passively-adaptive non-redundant legged robot whose stance and locomotion DOFs are decoupled via two identical 4-legged stance platforms connected by a 2-DOF planar mechanism [11]. The gait of the robot is as follows, assuming one of the platforms is on the ground: 1) the non-contact platform is translated / rotated relative to the stance platform, 2) the legs of the non-contact platform are lowered to make contact with the ground, and 3) the legs of the original stance platform are raised. This legged robot is designed to passively adapt to the terrain below it during the swing phase of locomotion, while remaining stable and fully-constrained during the stance phase. The use of four legs instead of three, which is the minimum required for static stability, serves to provide a more robust stance support pattern and corresponding stability margin [12].

The legs of the robot are 2-DOF serial chains of two revolute joints (RR) with parallel joint axes also parallel to the body plane (Fig. 2). They are controlled with a single input and are therefore underactuated; while there are several ways to actuate a 2-DOF leg with a single input, we choose to simply control the position of the proximal (hip) joint with a tendon and leave the distal (knee) joint passive with an elastic parallel mechanism connecting the distal link to the body of the robot. For more details on this leg design please see [8]. Our goal is to control all four legs with a single actuator, thereby controlling the height of the robot above ground.

We define the 4-RR stance platform with a set of kinematic design parameters (Fig. 3). Each leg is defined by the position of its hip relative to the origin (body center) in the x-y plane, h_i, the angle between the plane in which the foot moves and the x-axis, ϕ_i, and the lengths of the proximal and distal links. A specific platform configuration is also defined by the angles of the hip and knee joints, but for the purposes of the analysis below we will simply refer to the knee and foot locations in space as k_i and f_i, respectively. With these definitions we can proceed to analyze the mobility of the stance platform.

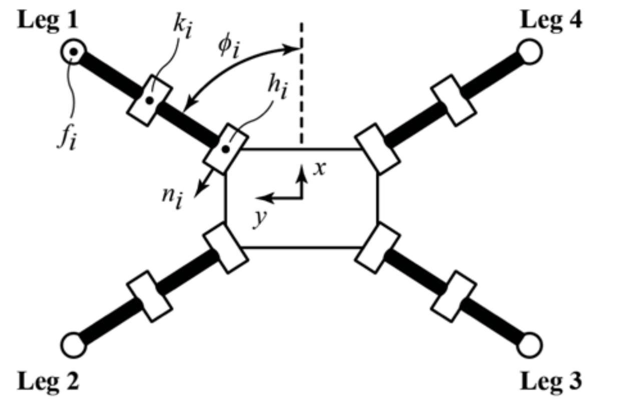

Figure 3. Diagram of the 4-RR stance platform with legs numbered and frame / leg parameters labeled.

III. Mobility Analysis and Actuation Schemes

In this section we use screw theory to analyze the mobility of the stance platform described in the previous section and identify any singular configurations. The mobility is used to determine the number of independent actuation constraints needed for the robot to be fully-constrained in stance, and several potential actuation schemes are presented.

A. Structural Mobility

One traditional method of determining the mobility of a given kinematic structure is the Chebychev-Grübler–Kutzbach (CGK) criterion [13], which simply takes into account structural parameters of the system, namely the number of rigid bodies, the number of joints, and the number of DOFs permitted by each joint in order to calculate the number of independent constraints necessary to define a configuration. It can take several equivalent forms, but we define it as:

$$m_{CGK} = 6(N - j - 1) + \sum_{i=1}^{j} f_i \tag{1}$$

where N is the number of rigid bodies (leg links, the robot body, and the ground in this case), j is the number of joints, and f_i is the number of DOFs permitted by joint i.

Taking the 4-RR stance platform presented in Section II and treating the ground contacts like spherical joints based on the point-contact with friction assumption [14], we find that $m_{CGK} = 6(10 - 12 - 1) + 20 = 2$. Therefore, in the general case, we could fully define the configuration of the platform (assuming the ground contact points are known) with two independent constraints, e.g. specifying the positions of any two revolute joints. However, the CGK criterion only provides a lower-bound on mobility [15]; in certain configurations, the specific location and orientation of the joints can result in constraint redundancy and the platform would gain additional DOFs. Evaluating these cases – essential for the control of the stance platform – requires a more in depth analysis, e.g. using group theoretic methods [16] or screw theory [17]; we adopt the latter approach.

B. Screw Theory Analysis

In order to evaluate the configuration-dependent mobility of the stance platform and identify singular configurations, we adopt the method presented in [18]. We define the motion-screw of a revolute joint located at point $\vec{r}$ with axis $\vec{v}$ as:

$$\$ = [\vec{v} \quad \vec{r}\times\vec{v}] \tag{2}$$

This can also represent the constraint-wrench of a force along $\vec{v}$ acting at $\vec{r}$. We also define two screws to be *reciprocal* to one another if their mutual moment vanishes, that is, when the following holds true:

$$\$_1 \circ \$_2 = \$_1^T \begin{bmatrix} 0 & I \\ I & 0 \end{bmatrix} \$_2 = 0 \tag{3}$$

where I is the 3×3 identity matrix. In physical terms, if a wrench and a screw are reciprocal to one another then the force/torque represented by the wrench does no work when acting along the motion described by the screw.

The general methodology, which can be applied to any kinematic topology for a stance platform, is as follows. First, we evaluate the motion-screw system of each leg, S_i, which is simply the union of all the joint screws, and describes the motion of the body permitted by the leg. We then find the constraint-screw system reciprocal to that screw system, i.e.

$$S_i^r = \{\$_1 | \$_1 \circ \$_2 = 0, \$_2 \in S_i\} \tag{4}$$

which describes the constraints imposed on the body by the leg. By taking the union of the leg constraint-screw systems we find the body constraint-screw system, which describes all of the constraints imposed on the body by the leg. The actual mobility of the system is equal to the rank of the body constraint-screw system; subtracting it from 6 gives us the platform mobility and taking the reciprocal of the body constraint-screw system gives us the specific motions DOFs permitted to the platform in that configuration.

For the case study, without loss of generality, we treat the spherical joint at the foot as three collocated revolute joints with orthogonal joint axes; combining that with the hip and knee joints we get the following motion-screw system for leg i (with positions h_i, k_i, and f_i as defined in Section II and letter subscripts representing coordinates, i.e. f_{xi} is the x-coordinate of f_i):

$$\begin{bmatrix} n_{xi} & n_{yi} & 0 & 0 & 0 & h_{xi}n_{yi} - h_{yi}n_{xi} \\ n_{xi} & n_{yi} & 0 & -k_{zi}n_{yi} & k_{zi}n_{xi} & k_{xi}n_{yi} - k_{yi}n_{xi} \\ 1 & 0 & 0 & 0 & f_{zi} & -f_{yi} \\ 0 & 1 & 0 & -f_{zi} & 0 & f_{xi} \\ 0 & 0 & 1 & f_{yi} & -f_{xi} & 0 \end{bmatrix} \tag{5}$$

This screw system is of rank 5, so we expect each leg to exert a single constraint on the body. Taking the reciprocal we get:

$$[1 \quad -ct_i \quad 0 \quad f_{zi}ct_i \quad f_{zi} \quad -f_{xi}ct_i - f_{yi}] \tag{6}$$

where $ct_i = \cot(\phi_i)$. This represents a pure force acting at foot along the direction of the leg normal. Combining the four leg constraint-screw systems we get:

$$S^r = \begin{bmatrix} 1 & -ct_1 & 0 & f_{z1}ct_1 & f_{z1} & -f_{x1}ct_1 - f_{y1} \\ 1 & -ct_2 & 0 & f_{z2}ct_2 & f_{z2} & -f_{x2}ct_2 - f_{y2} \\ 1 & -ct_3 & 0 & f_{z3}ct_3 & f_{z3} & -f_{x3}ct_3 - f_{y3} \\ 1 & -ct_4 & 0 & f_{z4}ct_4 & f_{z4} & -f_{x4}ct_4 - f_{y4} \end{bmatrix} \tag{7}$$

which, as expected, is of rank four in the general case, resulting in a kinematic mobility of two (two unique constraints required to fully constrain the system). We can identify a set of configurations where the rank of this system drops to three, requiring three independent constraints to be fully constrained.

The first problematic configuration occurs if $\cot(\phi_i)$ is constant for all four legs, i.e. they all act in parallel planes since $\cot(\theta) = \cot(\theta + \pi)$. In this case the second column of S^r is constant for all screws (along with the first and third columns), so this system is necessarily of rank three. The resulting body motion-screw system is:

$$S = \begin{bmatrix} 1 & 0 & 0 & 0 & 0 & 0 \\ 0 & 0 & 0 & 0 & 1 & 0 \\ 0 & 0 & 0 & 0 & 0 & 1 \end{bmatrix} \tag{8}$$

which corresponds to a body pitch about the x-axis, translation along the y-axis, and translation along the z-axis – in other words, planar motion.

The next problematic configuration occurs when all of the feet are the same distance from the body in the z-direction, i.e. $f_{zi} = f_z$. In this case the fifth column of S is constant for all screws, again resulting in a mobility of three. The resulting body motion-screw system is:

$$S = \begin{bmatrix} 1 & 0 & 0 & 0 & f_z & 0 \\ 0 & 1 & 0 & -f_z & 0 & 0 \\ 0 & 0 & 0 & 0 & 0 & 1 \end{bmatrix} \tag{9}$$

corresponding to rotation about axes parallel to the x- and y-axes on plane of the feet and translation along the z-axis.

Finally, we have constraint redundancy if the legs are radially distributed *and* the opposite feet are at the same distance from the body in the z-direction. If we multiply the first two screws of S^r by $-\sin(\phi_i)$ and the second two screws by $\sin(\phi_i)$, noting that scalar multiplication of screws does not affect the rank of the system, setting $\phi_1 = 0$, $\phi_2 = \pi/2$, $\phi_3 = \pi$, and $\phi_4 = 3\pi/2$, and setting $f_{z1} = f_{z3}$ and $f_{z2} = f_{z4}$ we get:

$$S^r = \begin{bmatrix} 0 & 1 & 0 & -f_{z1} & 0 & f_{x1} \\ -1 & 0 & 0 & 0 & -f_{z2} & f_{y2} \\ 0 & 1 & 0 & -f_{z1} & 0 & f_{x3} \\ -1 & 0 & 0 & 0 & -f_{z2} & f_{y4} \end{bmatrix} \tag{10}$$

This yields a body motion-screw system of:

$$S = \begin{bmatrix} 1 & 0 & 0 & 0 & f_{z1} & 0 \\ 0 & 1 & 0 & -f_{z2} & 0 & 0 \\ 0 & 0 & 0 & 0 & 0 & 1 \end{bmatrix} \tag{11}$$

which corresponds to rotation about the axis defined by feet 1 and 3, rotation about the axis defined by feet 2 and 4, and finally translation in the z-direction. Note that setting $f_{z1} = f_{z2}$ does not further reduce the rank of the constraint-screw system.

Based on the above, we should apply a minimum of three constraints to control the platform. While the first singular case, all legs parallel, is easy to avoid by appropriately selecting ϕ_i, the second case (e.g. flat ground) is much harder to avoid, and in fact would be a common terrain to encounter. While we will also choose ϕ_i such that the legs are not perfectly radially distributed, having an appropriate third constraint ensures that any instability or ill-conditioning that occurs as we approach any singular configuration is

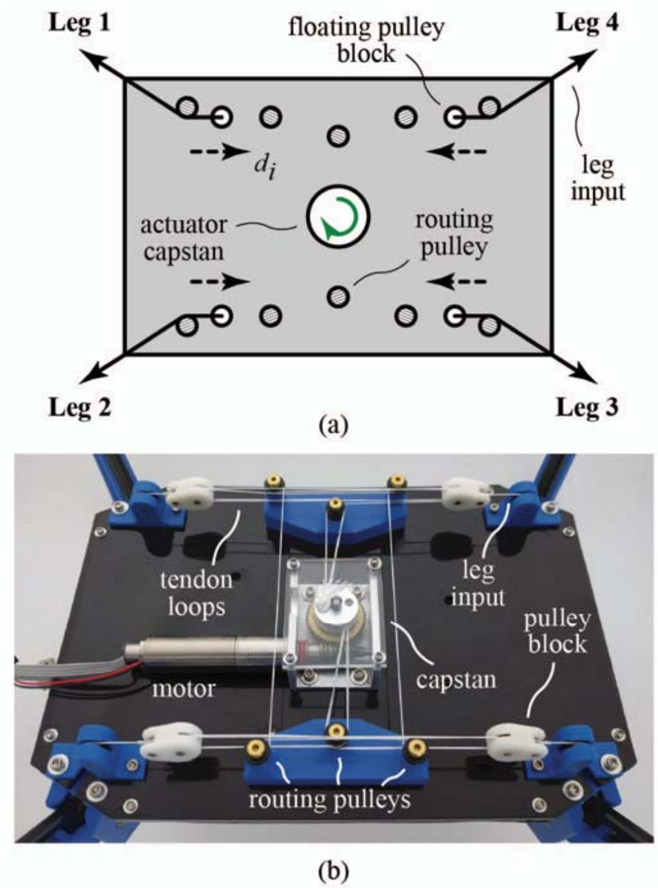

Figure 4. (a) Schematic of the components used to construct adaptive couplings with tendon loops connected to the single central actuator. (b) The physical implementation of an adaptive coupling scheme.

constrained. We now present several approaches for exerting at least three suitable independent constraints with a single actuator.

C. *Actuation Schemes*

We now turn to the problem of controlling four legs with a single actuator while exerting 3 independent constraints on the platform. As we mentioned previously, the legs are simply controlled by specifying the hip angle (Fig. 2), so we will treat them as a black box for the purpose of distributing the actuator effort. We define the leg excursion from its initial position for leg i as d_i and permit a single actuator to control all four legs by specifying relationships between the legs, as opposed to the specific positions of any one leg.

Adaptive couplings have been used with great success in the field of manipulation, implemented either through tendon couplings [7], linkages [19], or hydraulics / pneumatics [20]. Fig. 4 shows a schematic representation of the components of a tendon-driven actuation system as well as a real-world implementation, where loops of tendon are wrapped around pulley blocks that terminate the leg inputs and are themselves terminated on a central capstan. As the capstan rotates the size of the loop decreases, pulling both leg inputs and setting up a constraint of the form:

$$d_i + d_j \geq \ell \tag{12}$$

where ℓ is the change in size of the loop. The inequality comes from the fact that the tendon loop can only "pull", not push.

By turning the actuator to a specified position, we define the average excursion of the coupled joints. In our case studies, this is equivalent to the average distance of the feet of the coupled legs from the body. The coupled legs can still move, due to the underactuated nature of the coupling, but only in opposite directions, e.g. if leg i moves up, leg j must move down or the tendon constraint will not be satisfied. By definition, once any two feet are coupled together the body cannot translate (down) in the z-direction, since it would require both of those feet to move closer to the body.

We initially couple both pairs of opposite legs together with two tendon loops, as in Fig. 5a. This sets up the following two constraints:

$$\begin{aligned} d_1 + d_4 &\geq \ell \\ d_2 + d_3 &\geq \ell \end{aligned} \tag{13}$$

Note that since we use the same actuator / capstan for both tendon loops that the constraint value (ℓ) is the same for both pairs of legs. For a given actuator position, the average distance of both pairs of feet from the body is equal, and so in the absence of any external contacts or forces the legs all move simultaneously through a single actuator.

If we consider the feet, it is impossible for both foot 1 and foot 4 to move closer to the body (and similarly foot 2 and 3). Therefore, it is impossible for the body to roll about the y-axis (or any axis parallel to it) after contact, as such motion would violate the tendon constraints. Returning to (9) and (11), we see that these two couplings have constrained two out of the three permitted motions, but the body is still able to pitch about the x-axis.

In order to constrain the final body DOF we add a third coupling in parallel to the first two, coupling legs 3 and 4 together (Fig. 5b):

$$d_3 + d_4 \geq \ell \tag{14}$$

Combined with first two couplings, this prevents those two feet from moving closer to the body during stance and therefore prevents pitching in the "positive" direction about the x-axis based on the right hand rule. In order to exert three full constraints on the platform we must similarly couple legs 1 and 2 together, verifying that this does not violate the existing coupling constraints:

$$d_1 + d_2 = 2\ell - (d_3 + d_4) = \ell \tag{15}$$

One interesting consequence of this coupling scheme is that it necessarily requires *diagonally opposite* legs to be at equal positions, which can be demonstrated by setting the right sides of (13) and (14) equal to each other. While this was a component of the third singular configuration in the previous subsection, the fact that the system still has three independent constraints means that even in such a singular configuration the platform would still be stable.

For a given actuator position, the two pairs of opposite feet define two skew axes in space, parallel to the body plane, that are offset by some distance, ζ. By pitching and rolling the body while varying ζ, it is possible to guarantee that all four feet can make contact for arbitrary ground heights for each of the four feet. Another way to think about this is that the adaptive

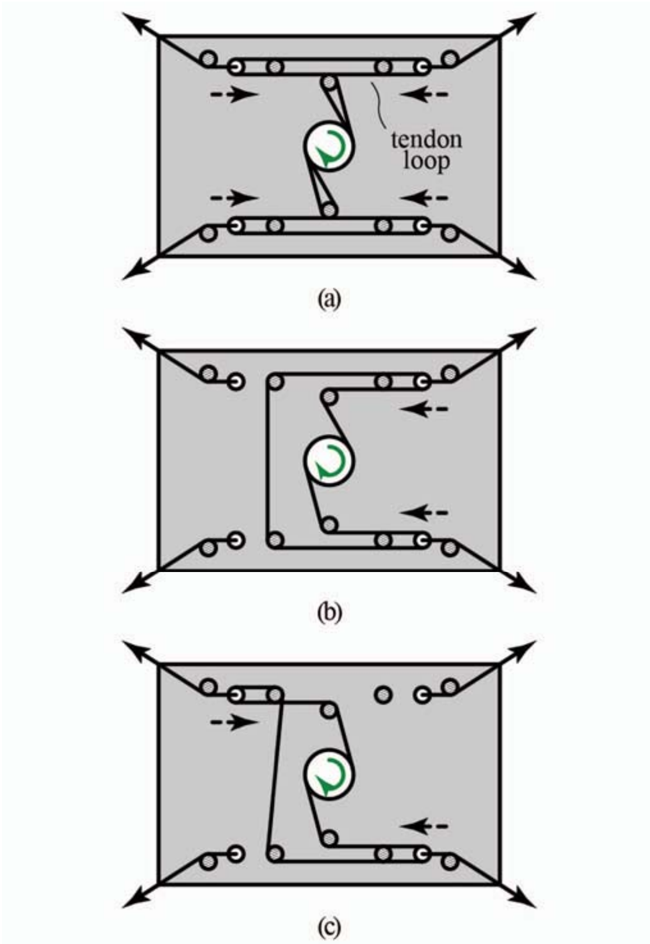

Figure 5. (a) Adaptive coupling connecting legs 1 / 4 and legs 2 / 3, exerting two constraints and serving as the base of our coupling scheme, meant to be paired with either (b) an adaptive coupling connecting legs 3 / 4 together or (c) an adaptive coupling connecting legs 1 / 3. Note that only (b) prevents the remaining body DOF and only in one direction, we combine it with a coupling between legs 1 / 2 to fully constrain the platform.

coupling permits arbitrary slopes between adjacent feet. In practice the adaptability will be bounded by the hard stops in the system, restricting it to guaranteed contact for some smaller set of ground height combinations. This will be further investigated in the following section.

We also considered coupling opposite legs together as in Fig. 5c. However, following the same analysis as above shows that this would result in legs 1 and 2 (and legs 3 and 4) necessarily being equal to each other. If the platform were to pitch about the x-axis those pairs of feet would effectively move together, and therefore that coupling does not actually exert an additional constraint on the platform.

An alternative method of controlling the platform is simply directly coupling all of the legs directly to the actuator, i.e. $d_1 = d_2 = d_3 = d_4$. This ends up exerting four independent constraints on the system, technically over-constraining it even near the previously identified singular configurations, but it does provide a baseline for the stance behavior of a four-legged platform.

TABLE I. SIMULATION DESIGN PARAMETERS

Parameter	Value
Body width	343 mm
Body length	320 mm
Minimum leg position	65 mm
Maximum leg position	227 mm
Elastic suspension travel	+0 / -16.2 mm
Maximum pitch / roll	Ā/2

IV. STANCE ANALYSIS

A. Simulation Model and Parameters

A numerical simulation was used to evaluate the stance performance of the different actuation schemes through the following metrics: a) if a platform could achieve stable stance, i.e. 3 or more feet in contact with the ground, b) if the platform could achieve full four-legged contact with the ground, c) what the approximate static stability margin [12] of the platform would be (distance from the COM projection and the edge of the projected support polygon in the global x-y plane), and d) what the platform inclination from level would be.. In short, it used a constrained optimization to find the body posture and position as well as the leg positions that would result in the lowest center-of-mass height given a set of terrain heights for each foot (implemented as an inequality constraint, e.g. $f_{zi} \geq height_i$). For the adaptively coupled actuation scheme, all four coupling constraints were set as inequality constraints.

Several simplifying assumptions were made for tractability. First, it was assumed that the body only had three permitted DOFs – translation in the z-direction, pitch about the x-axis, and roll about the y-axis, effectively assuming no slip at the ground contacts. Additionally, the legs were assumed to be 1-DOF prismatic joints acting along the body z-axis. In practice, the leg architecture shown in Fig. 1b results in foot motion that is approximately linear and parallel to the body normal due to the elastic linkage connecting the distal link to the body (assuming the proximal link is near the body plane). Once the feet are in contact with the ground, the extra DOF permits the robot to continue to change its height above ground without the feet slipping due to overconstraint. However, since the simulation completely ignored friction and neglected post-stance reconfiguration of the body, this overconstraint did not impact the validity of the results. Ultimately, the simulation attempted to find a kinematically valid configuration that minimized the center of mass height for arbitrary terrain heights.

A second reason to simplify the leg behavior was to avoid energetic effects on the results. In other words, had the passive knee with the elastic linkage been included, its spring stiffness would have added an additional parameter to the simulations that could have influenced the final stance configuration. By treating the leg as a 1-DOF prismatic joint, the problem was reduced to a matter of kinematics and geometry instead.

In addition to the adaptively coupled actuation scheme, two other actuation schemes were considered. First, the directly driven system was used as a base case. Second, a series elastic element was added to each leg in the form of a passive prismatic joint at the end, similar to an elastic suspension. In practice, the final positions of each passive joint would be a

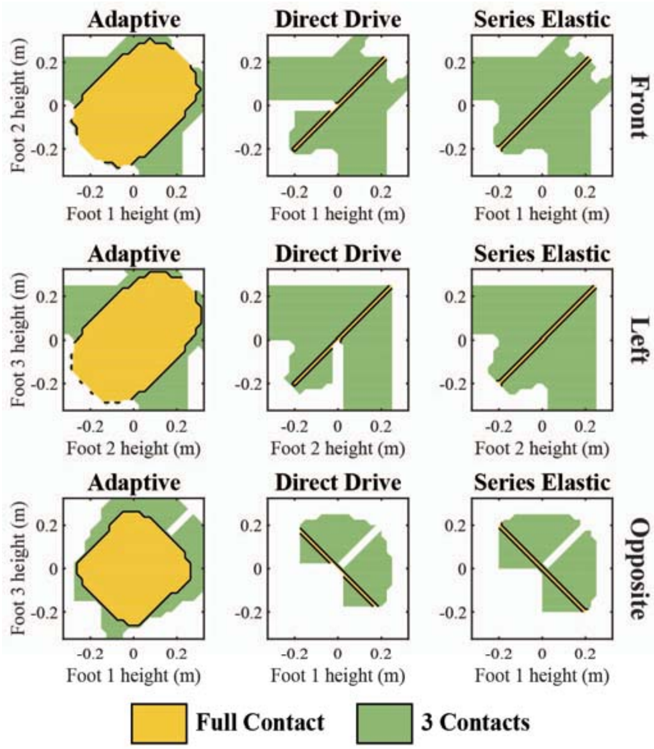

Figure 6. Contour plots showing the contact performance of the three actuation schemes, with the top row varying . The inner (yellow) regions represent full four-legged contact and the outer (green) regions represent three-legged contact. Note that the adaptive coupling scheme results in a dramatically larger region of full contact.

function of the spring stiffness used and the contact forces at each foot. To avoid this extra simulation parameter and its influence on the results, the joint was left entirely passive and simply given a range of motion equal to 10% of the overall leg range of motion.

The actual platform parameters were taken from the prototype platform used in the experimental validation (presented in the following section) and are shown in Table I. This included upper and lower hard stops for the leg position. The ground heights under each leg were varied between ± 325 mm with a step size of 25 mm, a range four times greater than the range of motion for each leg.

For each test case, the solver rejected any solution with fewer than 3 legs in contact or with an unstable stance (e.g. center of mass projection outside of the support pattern). If the solver converged on such a solution the limits on pitch/roll were gradually reduced to see if a kinematically valid solution existed with a higher center of mass. While this did not guarantee convergence to a valid solution, it helped reject invalid local minima. We will now present the results of varying the heights of two of the legs at a time.

B. Varying Two Feet

There were three unique situations in which the heights of the ground under two of the feet were held fixed (at zero) and the heights of the ground under the other two feet varied: a) varying legs 1 and 2 (the "front" feet, equivalent to 3 and 4 due to symmetry), b) varying legs 2 and 3 (the "left" feet, equivalent to 1 and 4), and c) varying legs 1 and 3 (the "opposite" feet, equivalent to 2 and 4). Fig. 6 shows the contact performance of the three actuation schemes across all three

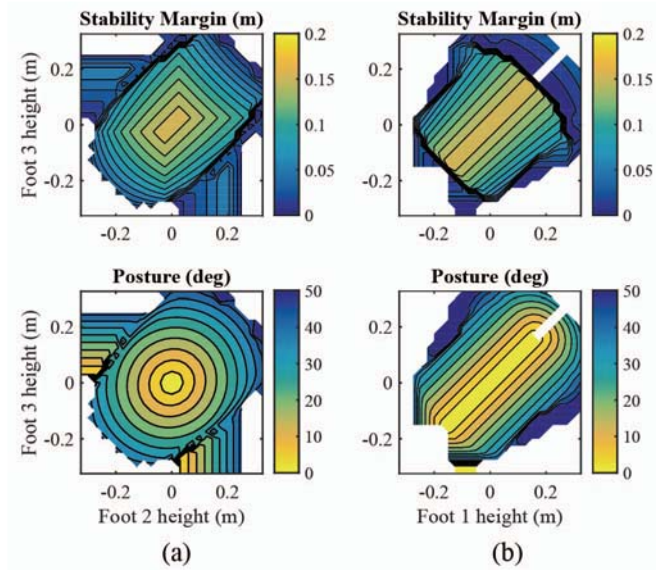

Figure 7. Stability margin and body posture contour plots for the adaptively coupled platform in (a) the "left" scenario and (b) the "opposite scenario. Note the relatively stable and level regions surrounding the origin.

scenarios. The adaptive coupling allows for a vastly larger region of full-contact as expected, and generally achieved a valid stance solution 75% of the time with full contact achieved 47% of the time, on average, across scenarios where the height differences were up to 300 mm between feet, double the average ground clearance of the platform.

In order to evaluate the quality of the stance configurations, the stability margin and body posture of the adaptively coupled platform was calculated and the "left" and "opposite" cases are shown in Fig. 7. The platform maintained a static stability margin above 50% of the maximum for 75% of the full contact cases and also maintained a body posture of less than 30 degrees for 75% of the full contact cases, maintaining both simultaneously for 72% of the full contact cases. Moreover, the adaptively coupled platform had a more level body than the series elastic platform in almost 87% of the comparable cases (where both made contact), averaging between 6 and 10.6 degrees improvement depending on the scenario.

C. Varying Three Legs

The full terrain space was explored by varying the terrain heights below legs 1, 2, and 3 across the same range as in the two-legged case, with the terrain under leg 4 kept at a height of zero. Since we were only concerned with the relative heights of the feet, not absolute, it was not necessary to explore the full 4-D space of foot heights to evaluate the overall stance performance of the platforms.

The adaptively coupled platform achieved full contact in 5,093 out of the total 19,683 test cases (26%). We should note that some of the full contact cases lay on the boundary of our terrain space, implying that the platform could have adapted to terrain with greater than a 0.325 m height difference between feet. 63% of the full contact cases maintained a stability margin above 50% of the maximum, 64% maintained body postures below 30 degrees, and 60% of the full contact cases met both criteria.

Fig. 8 shows body posture distributions for both the adaptively coupled platform and the directly driven platform, clearly showing a lower average body posture for the adaptive

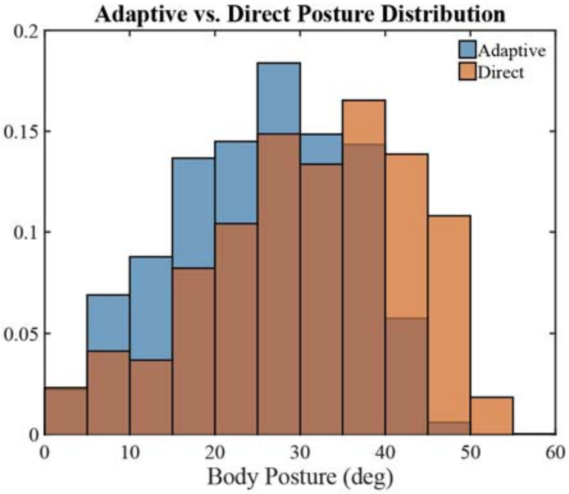

Figure 8. Simulated body posture distribution for the adaptive coupling vs the direct-drive platform. The adaptively coupled platform clearly results in lower body postures on average. Note that the color fill is transparent such that the adaptive distribution is visible underneath the direct distribution.

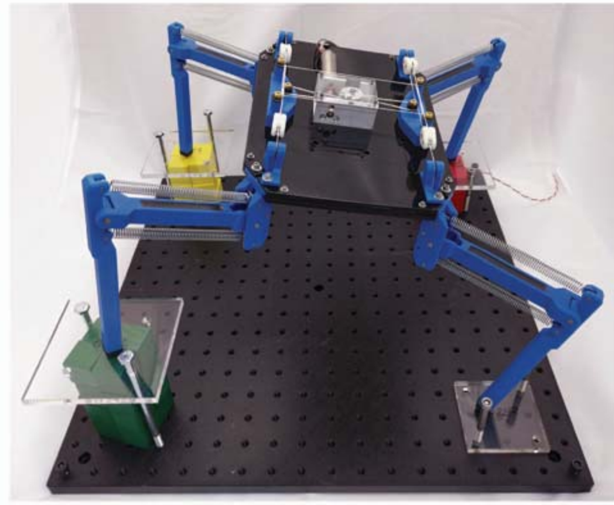

Figure 9. Picture of experimental setup – the adaptively coupled platform standing on "uneven terrain" with full contact.

platform. If we compare the postures of the two platforms at each test case, we find that the adaptively coupled platform maintained a more level posture 79% of the time, with an average improvement of 6.5 degrees.

Finally, the directly driven platform and the series elastic platform yielded very similar results. The series elastic case did achieve stable contact in 4.7% more test cases than the directly driven case but had a worse posture in 62% of comparable cases, albeit with an average difference of 0.4 degrees. It is clear that the inclusion of a more traditional suspension does not substantially change the adaptability and stance performance of a directly-driven stance platform.

V. Experimental Validation

A. Experimental Setup

Fig. 9 shows the experimental setup used to validate the simulation presented in Section IV. The body was constructed from 3 layered sheets of 3.175 mm Delrin and measured 240 mm by 165 mm. The legs were oriented at $\phi_1 = \pi/6$, $\phi_2 = 5\pi/6$, $\phi_3 = 7\pi/6$, and $\phi_4 = 11\pi/6$, with a proximal link length of 115 mm and a distal link length of 147 mm. They were primarily constructed from 3D-printed parts (Stratasys ABSplus) with a small foot cast from Smooth-On Vytaflex 30 urethane rubber. The elastic linkage was created using extension springs connecting the distal link to the hip mount of the body. The platform was actuated with a Maxon DCX 16L DC motor through a 44:1 planetary gearbox with an additional 48:1 worm drive to make the system non-backdrivable. We evaluated both the adaptively coupled and directly coupled platforms using 100 lb test PowerPro Spectra line as tendons. The adaptive coupling is shown in Fig. 4b.

The ground heights between each foot were set to either 0 mm, 50 mm, or 100 mm. Since this included leg 4, which always had a height of zero in the simulation, we were able to vary the effective height under each foot between $\pm$100 mm in increments of 50 mm for a total of 45 test cases. The terrain under each foot was emulated by placing a stack of 25 mm cubes on an optical breadboard, covered with a 3 mm sheet of acrylic. The latter was necessary due to the extremely low friction between the blocks – almost any lateral load would cause them to fall over. Finally, the body posture was recorded using a MicroStrain 3DM-GX3-25 inertial measurement unit.

In order to evaluate each test case, the platform was placed on a small stand and the legs were actuated to the position where the proximal links would be roughly straight out on level ground, which was sufficient to lift it off of the stand. The number of feet in contact were recorded, as were failed attempts, and a 3-second sample of the body posture was captured and the average recorded. We then subtracted the posture of the platform on level ground to offset variation in the construction of the tendon loops. Stance stability / robustness was evaluated by manually applying small lateral disturbances to the robot, e.g. pushing the body by hand, and seeing how it responded. A stance was considered stable if it moved minimally in response to the disturbance and returned to its original posture. Unstable stance occurred when the platform either fell over or moved easily in response to the disturbance. This was repeated for each of the 45 test cases and for both the adaptively coupled and directly coupled actuation schemes.

B. Results

On the whole, the experimental results largely matched the simulation results for both coupling schemes, but especially for the adaptively coupled platform, which was able to achieve full contact for all test cases. Moreover, the stance was fairly robust, with some small motion resulting from the disturbances but the platform returning to its original stance configuration. The postural measurements also matched the model, with no more than a 1.6 degree deviation from the simulation and an average deviation of 0.7 degrees, with the experiment generally less level than the simulation, likely due to mechanical slop in the joints causing the platform to sag slightly. Fig. 10 shows the experimental posture distributions, which generally matches the distributions in Fig. 8.

The directly coupled case was able to achieve full contact in 17 cases, three-legged stance in 14 cases, and it failed in the remaining 14 cases. Those failures were not strictly due to the kinematics of the system, but rather due to the passive knee joints and the ill-conditioned nature of the platform with only

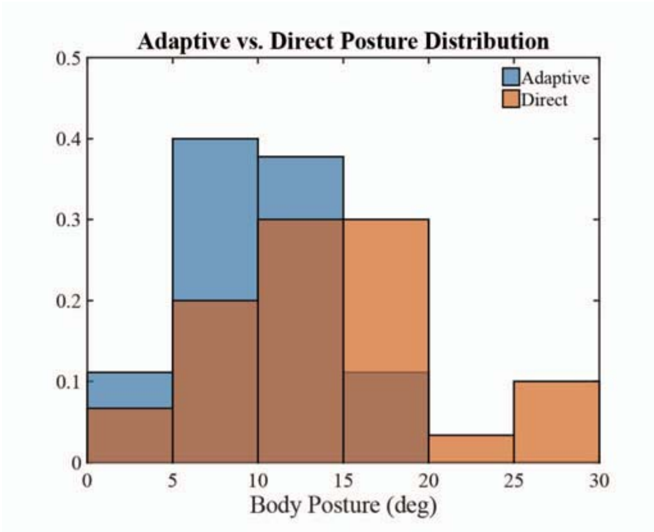

Figure 10. Experimental posture distributions for the adaptive and directly-coupled platforms; note the similarity to Fig. 8.

three contacts as discussed in [8]. Since opposite legs have parallel joint axes, they effectively form a 6-bar linkage with the ground when in stance. While the third leg should nominally constrain motion of that effective linkage, if the contact point of that leg is relatively far from the plane of the linkage, the slop in the joints and elasticity in the feet are sufficient to permit motion in the two parallel legs and the platform can tip over. That said, there were several cases where the simulation failed to find a full-contact configuration but it occurred in the experiment – we also attribute this to mechanical slop allowing the fourth leg to make contact.

The directly coupled platform deviated somewhat more from the simulation, with a maximum error of 11.4 degrees and an average error of 2.6 degrees. Generally, the experimental results were *more* level than the simulation, the cause of which remains unclear. Qualitatively, the 3-legged contacts were substantially less stable than full contact, with the platform primarily resting on the two opposite contact legs and easy to push towards the other side. The directly coupled platform did have a more angled posture than the adaptively coupled platform in 61% of the cases with an average difference of 4.1 degrees. Overall, the similar stance behaviors and postures seemed to validate the simulated results and definitely highlighted the robustness of the adaptively coupled actuation scheme in achieving full contact over varied terrain.

VI. Conclusions and Future Work

In this paper, we synthesize between-leg coupling schemes for passively-adaptive non-redundant legged robot, using a 4-RR platform as case study. Singular configurations of the stance platform are identified and the necessary number of constraints required to exactly-constrain the system are determined. Several parallel adaptive couplings are considered and the set that fully constrained the platform in stance is selected. A numerical simulation is performed to evaluate the stance performance of the coupling scheme as compared to a passive elastic suspension based on the number of contacts, body posture, and static stability margin. Simulation results demonstrate that the adaptively coupled platform is able to achieve full contact across a wide range of terrain types while maintaining a decent stability margin. It is also shown that the adaptive platform generally yields a slightly more level body posture than directly driven and series elastic platforms. The simulation is validated using a prototype stance platform, with the experimental results showing the high passive adaptability of the proposed solution.

Looking forward, we plan to build and test a complete system, specifically its ability to traverse and adapt to uneven terrain. We also plan to investigate the disturbance rejection and robustness of this robot more comprehensively.

Acknowledgment

The authors would like to thank Spencer Backus for his helpful discussions regarding both the platform design as well as the simulation.

References

[1] A. Roennau et al., "Design and kinematics of a biologically-inspired leg for a six-legged walking machine," in *2010 3rd IEEE RAS & EMBS International Conference on Biomedical Robotics and Biomechatronics*, 2010, pp. 626–631.
[2] R. Platt et al., "Null-Space Grasp Control: Theory and Experiments," *IEEE Trans. Robot.*, vol. 26, no. 2, pp. 282–295, Apr. 2010.
[3] M. R. Cutkosky and I. Kao, "Computing and controlling compliance of a robotic hand," *IEEE Trans. Robot. Autom.*, vol. 5, no. 2, pp. 151–165, Apr. 1989.
[4] M. Raibert et al., "BigDog, the Rough-Terrain Quadruped Robot," in *17th World Congress of the International Federation of Automatic Control*, 2008, pp. 10822–10825.
[5] M. P. Murphy et al., "The LittleDog robot," *Int. J. Rob. Res.*, vol. 30, no. 2, pp. 145–149, Dec. 2010.
[6] U. Saranli et al., "RHex: A Simple and Highly Mobile Hexapod Robot," *Int. J. Rob. Res.*, vol. 20, no. 7, pp. 616–631, Jul. 2001.
[7] A. M. Dollar and R. D. Howe, "The Highly Adaptive SDM Hand: Design and Performance Evaluation," *Int. J. Rob. Res.*, vol. 29, no. 5, pp. 585–597, Feb. 2010.
[8] O. Y. Kanner et al., "The Design of Exactly Constrained Walking Robots," in *2014 IEEE International Conference on Robotics & Automation*, 2014, pp. 2983–2989.
[9] P. Birkmeyer et al., "DASH: A dynamic 16g hexapedal robot," in *2009 IEEE/RSJ International Conference on Intelligent Robots and Systems*, 2009, pp. 2683–2689.
[10] S. Kim et al., "iSprawl: Design and Tuning for High-speed Autonomous Open-loop Running," *Int. J. Rob. Res.*, vol. 25, no. 9, pp. 903–912, Sep. 2006.
[11] O. Y. Kanner et al., "Design of a Passively-Adaptive Three Degree-of-Freedom Multi-Legged Robot With Underactuated Legs," in *ASME 2015 International Design Engineering Technical Conferences, Mechanisms and Robotics Conference*, 2015, p. V05AT08A062.
[12] E. Garcia et al., "A comparative study of stability margins for walking machines," *Robotica*, vol. 20, no. 6, Nov. 2002.
[13] K. H. Hunt, *Kinematic Geometry of Mechanisms*. London: Oxford University Press, 1978.
[14] J. K. Salisbury and J. J. Craig, "Articulated Hands: Force Control and Kinematic Issues," *Int. J. Rob. Res.*, vol. 1, no. 1, pp. 4–17, Mar. 1982.
[15] A. Müller, "Generic mobility of rigid body mechanisms," *Mech. Mach. Theory*, vol. 44, no. 6, pp. 1240–1255, Jun. 2009.
[16] Q. Li and J. M. Hervé, "1T2R Parallel Mechanisms Without Parasitic Motion," *IEEE Trans. Robot.*, vol. 26, no. 3, pp. 401–410, Jun. 2010.
[17] Z. Huang and Q. C. Li, "Type Synthesis of Symmetrical Lower-Mobility Parallel Mechanisms Using the Constraint-Synthesis Method," *Int. J. Rob. Res.*, vol. 22, no. 1, pp. 59–79, Jan. 2003.
[18] J. S. Dai et al., "Mobility of Overconstrained Parallel Mechanisms," *J. Mech. Des.*, vol. 128, no. 1, p. 220, 2006.
[19] L. Birglen, "Type Synthesis of Linkage-Driven Self-Adaptive Fingers," *J. Mech. Robot.*, vol. 1, no. 2, p. 21010, 2009.
[20] V. Begoc et al., "Mechanical design of a new pneumatically driven underactuated hand," in *2007 IEEE International Conference on Robotics and Automation*, 2007, pp. 927–933.